Abdominal Radiology

Published online: 10 November 2018

Abdom Radiol (2019) 44:1019–1026
https://doi.org/10.1007/s00261-018-1808-5

Rapid kVp switching dual-energy CT in the assessment of urolithiasis in patients with large body habitus: preliminary observations on image quality and stone characterization

Hamed Kordbacheh,[1] Vinit Baliyan,[1] Pranit Singh,[1] Brian H. Eisner,[2] Dushyant V. Sahani,[1] and Avinash R Kambadakone [1,3]

[1]Department of Radiology, Massachusetts General Hospital, Boston, MA, USA
[2]Department of Urology, Massachusetts General Hospital, Boston, MA, USA
[3]Department of Radiology, Massachusetts General Hospital, Harvard Medical School, 55 Fruit Street, White 270, Boston, MA 02114, USA

Abstract

Purpose: The purpose of this study was to investigate the image quality (IQ) considerations of rapid kVp switching dual-energy CT (rsDECT) in the assessment of urolithiasis in patients with large body habitus and to evaluate whether it allows stone characterization.

Materials and methods: In this IRB-approved, HIPAA compliant retrospective study, 93 consecutive patients (M/F = 72/21, mean age 56.9 years, range 23–83 years) with large body habitus (> 90 kg/198 lbs) who underwent dual-energy (DE) stone protocol CT on a rapid kVp switching DECT scanner between January 2013 and December 2016 were included. Scan acquisition protocol included an initial unenhanced single-energy CT (SECT) scan of KUB followed by targeted DECT in the region of stones. Two readers evaluated both CT data sets (axial 5 mm 120 kVp/140 kVp QC/70 keV monoenergetic, material density water/iodine images and coronal/sagittal 3 mm images) for the assessment of image quality (Scores: 1–4) and characterization of stone composition (reference standard: crystallography).

Results: One hundred and five CT examinations were performed in 93 patients (mean body weight 105.12 ± 13.53 kg, range 91–154 kg), and a total of 321 urinary tract calculi (mean size-4.8 ± 3.2 mm, range 1.2–22 mm) were detected. Both SECT and targeted monoenergetic images were of acceptable image quality (mean IQ: 3.77 and 3.83, kappa 0.79 and 0.87 respectively). Material density water and iodine images had lower IQ scores (mean IQ: 2.97 and 3.09 respectively) with image quality deterioration due to severe photon starvation/streak artifacts in 20% (21/105) and 17% (18/105) scans, respectively. Characterization of stone composition into uric acid/non-uric acid stones was achieved in 93.14% (299/321) of calculi (mean size: 4.99 ± 3.3 mm, range 1.2–22 mm), while 7% (22/321) stones could not be characterized (mean size 3.03 ± 1.16 mm, range 1.6–6.4 mm) ($p < 0.001$). Most common reason for non-characterization was image quality deterioration of the material density iodine images due to severe photon starvation artifacts. On multivariate regression, stone size and patient weight were predictors of stone composition determination on DECT ($p < 0.05$). The transverse diameter had a weak negative correlation with stone composition determination, but it was not statistically significant. Stone characterization into uric acid vs. non-uric acid stones was accurate in 95% ($n = 38/40$) of stones in comparison with crystallography.

Conclusion: In patients with large body habitus, rsDECT allowed characterization of most calculi (93%) despite image quality deterioration due to photon starvation/streak artifacts in up to 20% of material density images. Stone size and patient weight were predictors of stone composition determination on DECT, and small calculi in very large patients may not be characterized.

Hamed Kordbacheh and Vinit Baliyan are co-first authors.

Correspondence to: Avinash R Kambadakone; *email:* akambadakone@mgh.harvard.edu

Key words: Rapid kVp switching dual energy CT —Urolithiasis—Large body habitus

Rising incidence of obesity in the United States is a significant health-care burden with several adverse health effects [1]. Chronic illnesses such as diabetes, hypertension, hyperlipidemia and atherosclerotic disease have been directly linked to obesity [2]. Obesity is also considered a risk factor for urinary stone disease which has shown an increasing trend worldwide in patients of all body habitus [3–7]. The increased occurrence of urolithiasis in overweight or obese patients is multifactorial [7–11]. One of the factors contributing to the rising incidence of stone disease in obese patients is related to high intake of lithogenic substances such as oxalate and calcium [8]. This in conjunction with abnormal renal acid–base metabolism due to insulin resistance and low urinary pH in overweight/obese patients increases the risk of uric acid, calcium oxalate and calcium phosphate stones [12]. Obesity is associated with increased risk of gouty diathesis that often results in increased urinary uric acid excretion, an acidic urine environment and uric acid stone formation [11]. Additionally, bariatric surgical procedures performed to manage obesity are associated with hyperoxaluria and oxalate nephropathy [8]. Analogous to obesity, urinary stone disease has an adverse impact on the healthcare system related directly to the cost of stone treatment as well as the management of morbidity associated with their complications such as infection and chronic renal failure.

CT is the preferred modality for diagnosis and follow-up of stone disease, and therefore, appropriate management needs optimal CT scanning [13]. Imaging of patients with large body habitus increasingly poses complex challenges particularly in CT due to gantry size restrictions, need for precise patient positioning to avoid incomplete coverage of organs, image quality issues due to insufficient tube current and frequent occurrence of artifacts [3]. One of the unique contributions of DECT in management of patients with stone disease has been the improved ability to determine stone composition and therefore differentiate uric acid stones from non-uric acid stones [14]. Stone composition characterization allows triaging of patients to appropriate treatment strategy as uric acid stones can be treated medically initially while non-uric acid stones often need urologic intervention [13]. Presurgical determination of stone composition is particularly relevant in obese patients as they are difficult to respond to urological treatment, have higher complications, and there is emerging evidence that the association between urinary stones and obesity is stronger in patients with uric acid stones than in patients with calcium stones [15]. While DECT has substantial benefit in patients with large body habitus and is increasingly used in patients with urolithiasis, its feasibility in this patient population has not been reported with rapid kVp switching DECT platform. DECT for stone characterization is not routinely performed on the rsDECT platform in patients > 260 lbs (118 kg) due to concerns of image degradation and photon starvation limiting material decomposition. Consequently, the purpose of this study was to investigate the image quality considerations of rsDECT in the assessment of urolithiasis in patients with large body habitus and evaluate whether it allows stone characterization.

Materials and methods

Patient cohort and study design

This retrospective study was approved by Institutional Review Board (IRB) and Health Insurance Portability and Accountability Act (HIPAA) compliant. The need for informed consent was waived. We searched our radiology database using Render software, which acquires radiologic data from PACS workstations (AGFA Impax; AGFA Technical Imaging Systems, Ridgefield Park, NJ) to identify consecutive adult patients (≥ 18 years old) weighing > 90 kg (198 lbs) who underwent rapid kVp switching DECT scans for evaluation of stone disease (initial diagnosis or follow-up) from January 2013 to December 2016. Patient weight cut-off of > 90 kg instead of BMI was used as an inclusion criterion since this parameter is routinely recorded by CT technologists at the time of scanning for protocol selection, and is readily available from the radiology database and has been previously described in prior studies [16]. An additional subgroup within this cohort was identified to study DECT scanning in patients > 118 kg (260 lbs). The electronic medical records of the subjects were reviewed by an independent reviewer to document patient demographics and laboratory details (stone crystallography) if available.

DECT protocol and parameters

The subjects in the study cohort underwent a tailored stone protocol CT on a rsDECT scanner (GE Discovery CT 750 HD scanner, GE Healthcare, Milwaukee, WI, USA) (see Table 1 for protocol). The stone protocol CT acquisition at our institution includes an initial low-dose single-energy CT (SECT) scan extending from T12 vertebra to pubic symphysis followed by a targeted dual-energy CT acquisition performed in the region of stone. The parameters for the single-energy scan include: tube potential, 120 kVp; automated tube current modulation technique with a range of 150–450 mA; noise index, 26; section thickness, 5 mm; gantry rotation, 0.5 s; pitch, 1.375; detector configuration, 64 × 0.625 mm; and

Table 1. Single source DECT protocol

Parameter	Specification		
Dual energy mode	GSI		ROT/Body/MM/mA
		< 250 lbs	0.6/Med Body/40 mm/275 mA
		> 250 lbs	0.5/Med Body/40 mm/360 mA
kV	GSI		
Slice thickness	5 mm		
Interval	5 mm		
DFOV	Skin to skin		
Algorithm	Standard		
Pitch	1.375		
Speed	55		
ASIR	80%		

ASIR, adaptive statistical iterative reconstruction; DFOV, display field of view; GSI, gemstone spectral imaging; ROT, rotation time in second

Table 2. Image quality score per European Quality Criteria for CT

Diagnostic acceptability (DA)	Subjective analysis of image noise (SAN)	Presence of artifacts (PA)
1 = Unacceptable	1 = Too little or less than usual noise	1 = No artifact
2 = Acceptable only under limited conditions for visualization of abnormalities	2 = Acceptable noise	2 = Minor artifacts not affecting diagnostic interpretation
3 = Probably acceptable for interpretation	3 = Excessive noise	3 = Major artifacts affecting diagnostic interpretation
4 = Fully acceptable for diagnostic interpretation		4 = Artifacts rendering the study diagnostically unacceptable

adaptive statistical iterative reconstruction (ASIR) technique of 60%. The targeted DECT acquisition in the region of stone is performed by CT technologists trained to identify stones. The DECT protocol included 80 kVp/140 kVp simultaneous acquisition, 5 mm thickness and a tube rotation of 0.8–1 s for patients with large body habitus to ensure larger photon flux. For routine clinical practice, the following imaging data sets are typically generated for stone protocol CT—(a) axial 5 mm 120 kVp images, coronal 3 mm and sagittal 3 mm images from the initial SECT acquisition and (b) axial 5 mm 140 kVp QC, axial 5 mm 70 keV monoenergetic, axial 5 mm material density iodine (MD-I) and axial 5 mm material density water (MD-W) images from the targeted DECT acquisition. The image reconstruction was performed on the scanner console by the technologist. All the images were then transmitted to PACS workstation for diagnostic evaluation.

Qualitative analysis

The SECT and DECT imaging data sets were reviewed by two radiologists independently (5 and 15 years of experience) on a PACS workstation. The radiologists assessed the image data sets for image quality parameters based on European Quality Criteria for CT. A 4-point scale was used for diagnostic acceptability (DA: 4—fully acceptable for diagnostic interpretation, 3—probably acceptable for diagnostic interpretation, 2—acceptable only under limited conditions for visualization of abnormalities, 1—unacceptable). Subjective analysis of image noise (SAN) which refers to mottled appearance or graininess of images was rated on a scale of 1–3 (3—excessive noise, 2—acceptable noise, 1—too little or less than usual noise), and presence of image artifacts (PA) was rated on a scale of 1–4 (4—artifacts rendering the study diagnostically unacceptable, 3—major artifacts affecting diagnostic interpretation, 2—minor artifacts not affecting diagnostic interpretation, 1—no artifacts) (Table 2).

Quantitative analysis

Quantitative evaluation of stones included determination of stone size and stone location by an independent reader who was not involved in the qualitative analysis. The longest linear measurement of stone size was estimated using routine window settings. The location of the stones in the urinary tract (kidney, renal pelvis, ureter and urinary bladder) was documented. Objective image noise was calculated by placement of region of interest (ROI) in the subcutaneous fat at the level of the kidneys for the 70 keV monoenergetic images. Objective image noise was defined as the standard deviation of the attenuation

values within the ROI. The transverse diameter of all the patients was estimated on the axial image data sets at the level of kidneys using electronic calipers on PACS workstation.

Stone composition characterization

The MD-W and MD-I images were evaluated for determination of stone composition to differentiate between uric acid and non-uric acid stones based on 2-material decomposition algorithm. Uric acid stones have lower atomic number (effective atomic number: 6.9), while non-uric acid stones have higher atomic number (effective atomic number: 9.7–14) leading to different degrees of Compton and photoelectric interaction at high (140 kVp) and low (80 kVp) energies [17]. Since water and iodine span the atomic number range of the material generally found in CT imaging, the low (water) and high (iodine) atomic number material are selected as basis pair for 2-material decomposition algorithm on rsDECT [17]. Therefore, a stone visible on MD-W image but not on MD-I image was characterized as uric acid stone, and on the other hand, the stone perceptible on both MD-W and MD-I images was considered a non-uric acid stone [17]. The appearance of mixed stone on the MD-I and MD-W images was dependent on its dominant composition. For example, a dominant uric acid component would be imperceptible on MD-I, but a minor non-uric acid component would be visible [17]. This assessment of stone characterization was done by a consensus read from both readers. In those patients who underwent definitive treatment for stone extraction, crystallographic analysis of the extracted stones was used to determine stone composition using semiquantitative polarizing microscopy with infrared spectrophotometry. Crystallographic analysis formed the reference standard for stone composition characterization.

Statistical analysis

Microsoft Excel 2007 (Microsoft Corporation) and MedCalc software (version 18.2.1, Ostend Belgium) were used for statistical analysis. Simple linear regression was performed for the correlation of image quality parameters and body weight. The average image quality scores for the two readers were estimated. *Kappa statistics*—inter-observer agreement was used for image quality parameters. The K value can be interpreted as follows: poor (< 0.20), fair (0.21–0.40), moderate (0.41–0.60), good (0.61–0.80) and very good (0.81–1.00). Regression analysis was used to describe the relation between mean image quality parameters and patient weight. Multivariate regression was also performed to find the independent predictors of characterizability. The factors considered for multivariate analysis included stone size, stone location, body weight and transverse diameter. The p values < 0.05 were considered as statistically significant.

Results

Patient demographics

The final patient cohort consisted of 93 patients (M: F = 72/21, mean age: 56.9 years, range 23–83 years) who underwent a total of 105 DECT scans. A total of 321 urinary tract calculi (mean size 4.8 ± 3.2 mm, range 1.2–22 mm) were detected in 92 out of 105 examinations. The mean patient body weight was 105.12 ± 13.53 kg (range 91–154 kg). The average transverse diameter was 415 ± 40 mm (range 354–500 mm). A total of 36 stones were detected in 14 patients > 260 lbs (118 kg) with mean size 5.71 ± 3.68 mm (range 2–19.5 mm).

Image quality

Mean image quality parameters showed poor correlation with patient weight (R Squared range: 0.03–0.29). Both the single energy CT and the targeted anatomy monoenergetic images were of acceptable image quality for interpretation (mean DA score = 3.77 for SECT and 3.83 for monoenergetic images) with good to excellent inter-observer agreement (kappa = 0.79 and 0.87 for SECT and monoenergetic images, respectively).

Overall, the MD-W and MD-I images had acceptable image quality for interpretation (mean diagnostic acceptability = 2.97 and 3.09, respectively) with good inter-observer agreement (kappa = 0.68 and 0.73, respectively) (Table 3). However, MD-W and MD-I images suffered from clinically significant artifacts (PA ≥ 3/4) in 20% (21/105) and 17% (18/105) scans, respectively. The image quality of MD-W and MD-I was below fully diagnostic (≤ 2/4) in 22% (23/105) and 20% (21/105) scans, respectively. The MD-W was non-diagnostic in 4% (4/105) scans, while MD-I was non-diagnostic in 6% scans (6/105). The subjective image noise and artifact scores for monoenergetic images were 1.48 and 1.14, suggesting image quality parameters conducive for diagnosis (Table 3). Mean image quality parameters for both the water images and iodine showed poor correlation with patient weight (R Squared range: 0.13–0.20) (Table 4).

Quantitative analysis and stone characterization

Characterization of stone composition into uric acid/non-uric acid stones (calcium, $n = 284$ uric acid, $n = 11$, and mixed, $n = 4$ was achieved in 93.14% (299/321) of calculi (mean size 4.99 ± 3.3 mm, range

Table 3. Image quality scores for DECT data sets

	Mono (70 keV) (n = 105)			SECT (120 kVp) (n = 105)			Water (n = 105)			Iodine (n = 105)		
	DA	PA	SAN	DA	PA	SAN	DA	PA	SAN	DA	PA	SAN
Reader A	3.82 (r = 2–4) ($\leq$ 2 in 3)*	1.14 (r = 1–3) ($\geq$ 3 in 3)	1.48 (r = 1–3) ($>$ 2 in 4)	3.74 (r = 2–4) ($\leq$ 2 in 1)	1.20 (r = 1–3) ($\geq$ 3 in 1)	1.61 (r = 1–3) ($>$ 2 in 9)	2.94 (r = 1–4) ($\leq$ 2 in 25, in 4 cases = 1)	2.08 (r = 1–4) ($\geq$ 3 in 25)	1.95 (r = 1–3) ($>$ 2 in 16)	3.04 (r = 1–4) ($\leq$ 2 in 24, in 7 cases = 1)	2.12 (r = 1–4) ($\geq$ 3 in 26)	1.87 (r = 1–3) ($>$ 2 in 13)
Reader B	3.83 (r = 2–4) ($\leq$ 2 in 3)	1.14 (r = 1–3) ($\geq$ 3 in 3)	1.49 (r = 1–3) ($>$ 2 in 6)	3.80 (r = 2–4) ($\leq$ 2 in 1)	1.28 (r = 1–3) ($\geq$ 3 in 1)	1.58 (r = 1–3) ($>$ 2 in 9)	3 (r = 1–4) ($\leq$ 2 in 28, in 5 cases = 1)	2.12 (r = 1–4) ($\geq$ 3 in 29)	1.91 (r = 1–3) ($>$ 2 in 20)	3.14 (r = 1–4) ($\leq$ 2 in 20, in 7 cases = 1)	2.04 (r = 1–4) ($\geq$ 3 in 20)	1.81 (r = 1–3) ($>$ 2 in 16)
Mean	3.83 (r = 2–4) ($\leq$ 2 in 3)	1.14 (r = 1–3 ($\geq$ 3 in 3)	1.48 (r = 1–3) ($>$ 2 in 4)	3.77 (r = 2–4) ($\leq$ 2 in 1)	1.24 (r = 1–3) ($\geq$ 3 in 1)	1.59 (r = 1–3) ($>$ 2 in 9)	2.97 (r = 1–4) ($\leq$ 2 in 23, in 4 cases = 1, 1 case = 1.5)	2.10 (r = 1–4) ($\geq$ 3 in 21)	1.93 (r = 1–3) ($>$ 2 in 20)	3.09 (r = 1–4) ($\leq$ 2 in 21, in 6 cases = 1, 1 case = 1.5)	2.08 (r = 1–4) ($\geq$ 3 in 18)	1.84 (r = 1–3) ($>$ 2 in 16)
Kappa	0.87	0.70	0.72	0.79	0.75	0.75	0.68	0.77	0.67	0.73	0.74	0.69

SECT, single energy CT
*The numbers in parenthesis refers to DA $\leq$ 2, PA $\geq$ 3, and SAN $>$2. These numbers have been reported because these are the IQ thresholds depicting significant limitation of IQ, which has a potential for affecting the diagnostic interpretation

1.2–22 mm), while stone characterization was not possible in 6.8% (22/321) of stones (mean size: 3.03 ± 1.16 mm, range 1.6–6.4 mm) ($p < 0.01$). Photon starvation/streak artifacts limited or obscured visualization of stones either on MD-W or MD-I images or both. In these situations, stones visible on MD-I images and obscured on MD-W images were characterized as non-uric acid. Stones obscured on MD-I images only or on both MD-W and MD-I images were considered as uncharacterizable. Crystallographic results of stone composition were available in 40 patients, and DECT allowed stone composition determination in 38 (95%) of these patients. In these patients, the stone composition determined by DECT was concordant with the crystallographic results (35 calcium stones and 3 uric acid).

On multivariate regression, stone size and patient weight came out as a predictor for ability to characterize the stone ($p < 0.005$ and < 0.05, respectively). The transverse diameter had a weak negative correlation with stone characterization, but it was not statistically significant ($p = 0.41$) (Tables 5, 6). There were 36 calculi (size 5.71 ± 3.68 mm) in patients > 118 kg (260 lbs), out of these 31 calculi (6.05 ± 3.85 mm) could be characterized. The size of uncharacterized stones was 3.58 ± 0.54 mm (range 2.9–4.1 mm) in this subgroup (Fig. 1).

Discussion

Stone composition characterization prior to urological intervention has substantial impact on management as patients with uric acid calculi are often treated by non-surgical options including urinary alkalization [18, 19]. Therefore, there is increasing demand for obtaining this information from MDCT scans in patients with urolithiasis. Stone characterization on MDCT has evolved from measurement of attenuation values on single-energy CT to using robust methods such as material decomposition on DECT [20–23]. While DECT has been established to allow accurate characterization of stone composition in both phantom and human studies, there is limited literature on its value in patients with large body habitus [24, 25]. Increasing occurrence of both uric acid and calcium stones in obese patients necessitates accurate pretreatment determination of stone composition as these patients pose unique challenges to urological intervention due to their body habitus [26]. Expert opinion and vendor recommendations often limit DECT scanning in patients > 260 lbs (118 kg) due to concerns of inaccurate material decomposition due to effects of photon starvation. In our cohort of patients with large body habitus, we found that stone protocol rsDECT resulted in limited image quality of material specific images in up to 20% of scans. However, despite these artifacts and inferior image quality, the diagnostic interpretation and stone charac-

Table 4. Linear regression analysis of mean image quality parameters and patient weight

Image quality parameters	Mono (70 keV)			SECT			Water			Iodine		
	DA	PA	SAN	DA	PA	SAN	DA	PA	SAN	DA	PA	SAN
R^2	0.29	0.29	0.19	0.04	0.15	0.03	0.13	0.08	0.12	0.20	0.15	0.14
p value	< 0.001	< 0.001	< 0.001	< 0.001	< 0.001	< 0.001	< 0.001	< 0.01	< 0.001	< 0.001	< 0.001	< 0.001

Table 5. Multiple regression (characterizability)

Variables	Coefficient	$r_{partial}$ (corrected coefficient)	p value
Diameter	− 0.0007572	− 0.04827	0.4104
Location	0.09265	0.07595	0.1949
Size	0.02415	0.1653	0.0046
Weight	− 0.006750	− 0.1172	0.0450

Table 6. Image quality scores for DECT data sets in patients > 260 lbs, mean (95% CI for the arithmetic mean)

	DA	PA	SAN
Mono (70 keV)	3.21 (2.76–3.66)	1.67 (1.21–2.14)	1.96 (1.54–2.37)
SECT 120 kVp	3.53 (3.27–3.8)	1.67 (1.43–1.92)	1.82 (1.53–2.11)
Iodine	2.14 (1.61–2.66)	2.96 (2.41–3.51)	2.42 (2.05–2.80)
Water	2.32 (1.73–2.90)	2.71 (2.12–3.29)	2.39 (2.01–2.77)

terization were largely not impacted. Our study results also show that stone size and patient weight were independent predictors of stone characterization in patients with large body habitus on rsDECT platform.

We found that image quality of initial single-energy CT scans was within diagnostic range across different body sizes in patients > 90 kg (198 lbs). The rsDECT platform uses ASIR, a statistical iterative reconstruction technique to diminish image noise and artifacts to enhance image quality and remove excessive graininess from images [27, 28]. Several authors have reported that iterative reconstruction techniques from various MDCT technologies are effective in enhancing image quality and reducing image noise in patients across all weight categories including patients with large body habitus [27–33].

Our imaging findings are consistent with the prior experience with non-obese patients where the small stone characterization (< 3 mm) has been reported to be less accurate [25, 34–38]. Our study showed the average size of stones uncharacterizable by DECT to be 3.03 mm in patients ≥ 90 kg (198 lbs). Qu et al. investigated characterization of stones in large body habitus based on a phantom and patient study using the dual source DECT scanner [24]. They reported that dual source DECT could provide determination of stone composition for patients with a wide range of body sizes using a phantom model (body phantom with dimensions of 30–50 cm) and patients (28–50 cm diameter). Qu and colleagues did not assess the impact of body habitus on subjective image quality and did not compare findings among different body sizes. Moreover, this study was performed using a dual source DECT scanner (dsDECT). Qu et al. found that image noise increased with increasing patient size but was within acceptable limits in all cases. This study did not report a high incidence of photon starvation artifacts with enlarging body size. The differences in DECT technology between the rsDECT and dual source DECT scanners could possibly explain this difference. Due to use of a rapid kVp switching between low and high voltages, rsDECT scanners does not allow performance of angular tube current modulation and use a fixed current over entire rotation [39]. With larger body habitus and obesity, the transverse diameter may increase disproportionately in supine position [40], and the beam energy may not get enough penetration in this direction and could have possibly resulted in the artifacts. As dsDECT allows angular tube current modulation, photon starvation may not be so much apparent with this technique [24]. Photon starvation could also be result of limited maximum tube current output that could be obtained from the rsDECT platform.

Our study had few limitations including that this was a retrospective single center study with potential for over-estimation bias and lack of power analysis of study sample size. Our study findings were designed to allow characterization of stone composition into uric acid and non-uric acid stones. Additional characterization of stone composition based on z-effective number and charts was not attempted in this preliminary study since additional post-processing would need to be performed on dedicated post-processing workstation which is not part of our routine clinical workflow. Our intent in this study was to investigate routine characterization of stone composition based on material density image data sets available on PACS without need for additional post-processing which reflected the routine workflow. Reference standard comparison of stone crystallographic analysis results was not available in all patients. Nevertheless, in those patients with available stone composition results by crystallography, there was high degree of concordance with rsDECT results. The diagnostic accuracy of the radiologists in detecting stones was not tested in this study. Finally, the stone composition characterization in our patients with large body habitus was not compared with the diagnostic performance in patients

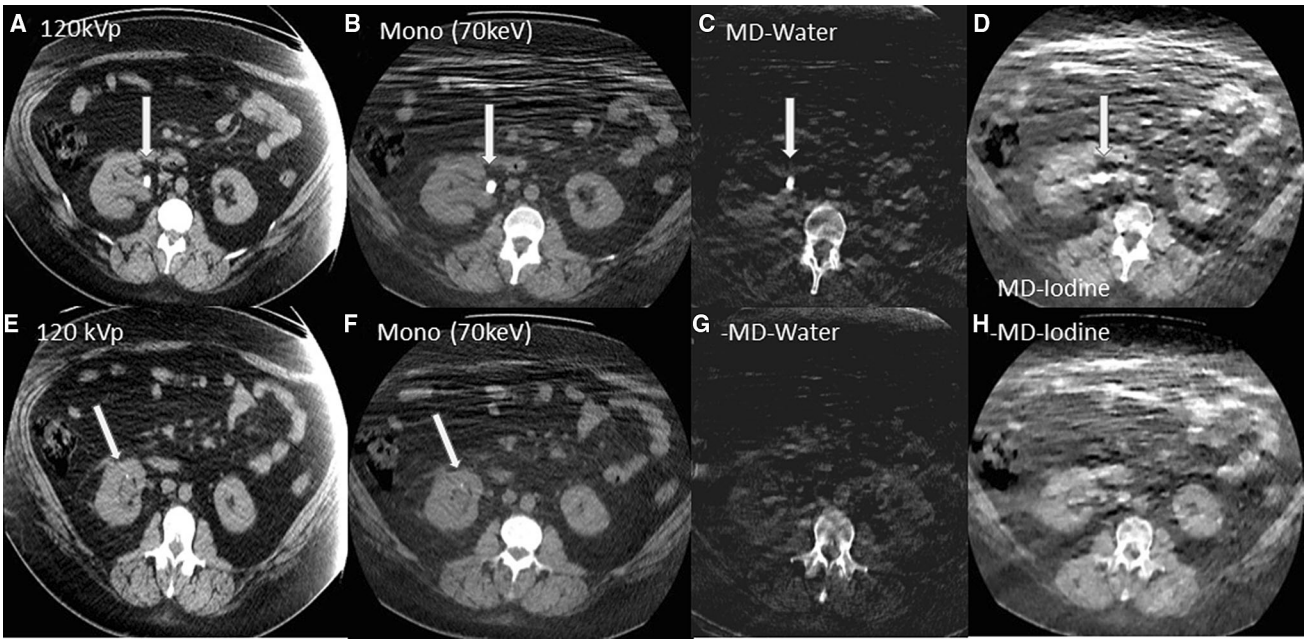

Fig. 1. Stone characterization using rsDECT in a patient with large body habitus (weight = 154 kg). Axial non-contrast 120kVp single-energy CT (**A**) and axial 70 keV monoenergetic (**B**) images at the level of renal pelvis show a 11-mm calculus which is characterized as calcium containing stone as it is visible on both MD-W (**C**) and MD-I (**D**) images despite significant photon starvation and streak artifacts in these images. The bottom panel shows axial non-contrast 120 kVp single-energy CT (**E**) and axial 70 keV monoenergetic (**F**) images at the level of lower pole where a punctate 2-mm calculus cannot be characterized because it is not visible on MD-W (**G**) or MD-I images (**H**) due to significant streak and photon starvation artifacts on these images.

with body weight < 90 kg and we relied on the published literature for this comparison.

Conclusion

In patients with large body habitus, rsDECT allowed characterization of most calculi (93%) despite image quality deterioration due to photon starvation/streak artifacts in up to 20% of material density images. Stone size and patient weight were predictors of stone composition determination on DECT, and small calculi in very large patients may not be characterized.

Compliance with ethical standards

Funding There is no source of funding for this original article. The author identifying information is on the title page that is separate from the manuscript.

Conflict of interest Hamed Kordbacheh, MD, declares he has no conflict of interest; Vinit Baliyan, MD, declares he has no conflict of interest; Pranit Singh declares he has no conflict of interest; Brian H Eisner, MD, declares he has no conflict of interest; Dushyant V Sahani, MD, recieves grant support for research activities from GE healthcare, Advisory Board of Allena Pharmaceuticals, Royalties from Elsevier; Avinash R Kambadakone, MD, FRCR, declares he has no conflict of interest.

Ethical approval This article does not contain any studies with human participants or animals performed by any of the authors.

References

1. Sturm R, Hattori A (2013) Morbid obesity rates continue to rise rapidly in the US. Int J Obes 2005. 37(6):889–891
2. Jarolimova J, Tagoni J, Stern TA. Obesity: its epidemiology, comorbidities, and management. prim care companion CNS Disord. 2013; 15(5). https://www.ncbi.nlm.nih.gov/pmc/articles/PMC3907314/. Accessed 31 Mar 2018
3. Uppot RN, Sahani DV, Hahn PF, et al. (2006) Effect of obesity on image quality: fifteen-year longitudinal study for evaluation of dictated radiology reports 1. Radiology. 240(2):435–439
4. Scales CD, Smith AC, Hanley JM, Saigal CS (2012) Urologic diseases in America project. Prevalence of kidney stones in the United States. Eur Urol 62(1):160–165
5. Pak CY, Sakhaee K, Peterson RD, Poindexter JR, Frawley WH (2001) Biochemical profile of idiopathic uric acid nephrolithiasis. Kidney Int. 60(2):757–761
6. Ekeruo WO, Tan YH, Young MD, et al. (2004) Metabolic risk factors and the impact of medical therapy on the management of nephrolithiasis in obese patients. J Urol. 172(1):159–163
7. Semins MJ, Shore AD, Makary MA, et al. (2010) The association of increasing body mass index and kidney stone disease. J Urol. 183(2):571–575
8. Carbone A, Al Salhi Y, Tasca A, et al. (2018) Obesity and kidney stone disease: a systematic review. Minerva Urol E Nefrol Ital J Urol Nephrol. 70(4):393–400
9. Najeeb Q, Masood I, Bhaskar N, et al. (2013) Effect of BMI and urinary pH on urolithiasis and its composition. Saudi J Kidney Dis Transplant. 24(1):60–66
10. Chou Y-H, Su C-M, Li C-C, et al. (2011) Difference in urinary stone components between obese and non-obese patients. Urol Res. 39(4):283–287
11. Daudon M, Traxer O, Conort P, Lacour B, Jungers P (2006) Type 2 diabetes increases the risk for uric acid stones. J Am Soc Nephrol JASN. 17(7):2026–2033

12. Hess B (2012) Metabolic syndrome, obesity and kidney stones. Arab J Urol. 10(3):258–264
13. Brisbane W, Bailey MR, Sorensen MD (2016) An overview of kidney stone imaging techniques. Nat Rev Urol. 13(11):654–662
14. McCarthy CJ, Baliyan V, Kordbacheh H, et al. (2016) Radiology of renal stone disease. Int J Surg Lond Engl. 36(Pt D):638–646
15. Daudon M, Lacour B, Jungers P (2006) Influence of body size on urinary stone composition in men and women. Urol Res. 34(3):193–199
16. Megibow AJ, Sahani D (2012) Best practice: implementation and use of abdominal dual-energy CT in routine patient care. AJR Am J Roentgenol. 199(5 Suppl):S71–S77
17. Kulkarni NM, Eisner BH, Pinho DF, et al. (2013) Determination of renal stone composition in phantom and patients using single-source dual-energy computed tomography. J Comput Assist Tomogr. 37(1):37–45
18. Ngo TC, Assimos DG (2007) Uric acid nephrolithiasis: recent progress and future directions. Rev Urol. 9(1):17–27
19. Caramia G, Di Gregorio L, Tarantino ML, et al. (2004) Uric acid, phosphate and oxalate stones: treatment and prophylaxis. Urol Int. 72(Suppl 1):24–28
20. Duan X, Li Z, Yu L, et al. (2015) Characterization of urinary stone composition by use of third-generation dual-source dual-energy CT with increased spectral separation. AJR Am J Roentgenol. 205(6):1203–1207
21. Leng S, Huang A, Cardona JM, et al. (2016) Dual-energy CT for quantification of urinary stone composition in mixed stones: a phantom study. Am J Roentgenol. 207(2):321–329
22. Wisenbaugh ES, Paden RG, Silva AC, Humphreys MR (2014) Dual-energy vs conventional computed tomography in determining stone composition. Urology. 83(6):1243–1247
23. Akand M, Koplay M, Islamoglu N, et al. (2016) Role of dual-source dual-energy computed tomography versus X-ray crystallography in prediction of the stone composition: a retrospective non-randomized pilot study. Int Urol Nephrol. 48(9):1413–1420
24. Qu M, Jaramillo-Alvarez G, Ramirez-Giraldo JC, et al. (2012) Urinary stone differentiation in patients with large body size using dual-energy dual-source computed tomography. Eur Radiol. 23(5):1408–1414
25. Jepperson MA, Cernigliaro JG, Sella D, et al. (2013) Dual-energy CT for the evaluation of urinary calculi: image interpretation, pitfalls and stone mimics. Clin Radiol. 68(12):e707–e714
26. Le NTT, Robinson J, Lewis SJ (2015) Obese patients and radiography literature: what do we know about a big issue? J Med Radiat Sci. 62(2):132–141
27. Desai GS, Fuentes Orrego JM, Kambadakone AR, Sahani DV (2013) Performance of iterative reconstruction and automated tube voltage selection on the image quality and radiation dose in abdominal CT scans. J Comput Assist Tomogr. 37(6):897–903
28. Desai GS, Uppot RN, Yu EW, Kambadakone AR, Sahani DV (2012) Impact of iterative reconstruction on image quality and radiation dose in multidetector CT of large body size adults. Eur Radiol. 22(8):1631–1640
29. Shaqdan KW, Kambadakone AR, Hahn P, Sahani DV (2018) Experience with iterative reconstruction techniques for abdominopelvic computed tomography in morbidly and super obese patients. J Comput Assist Tomogr. 42(1):124–132
30. Soenen O, Balliauw C, Oyen R, Zanca F (2017) Dose and image quality in low-dose CT for urinary stone disease: added value of automatic tube current modulation and iterative reconstruction techniques. Radiat Prot Dosimetry. 174(2):242–249
31. Andrabi Y, Pianykh O, Agrawal M, et al. (2015) Radiation dose consideration in kidney stone CT examinations: integration of iterative reconstruction algorithms with routine clinical practice. AJR Am J Roentgenol. 204(5):1055–1063
32. Desai GS, Thabet A, Elias AYA, Sahani DV (2013) Comparative assessment of three image reconstruction techniques for image quality and radiation dose in patients undergoing abdominopelvic multidetector CT examinations. Br J Radiol. 86(1021):20120161
33. Prakash P, Kalra MK, Kambadakone AK, et al. (2010) Reducing abdominal CT radiation dose with adaptive statistical iterative reconstruction technique. Invest Radiol. 45(4):202–210
34. Eliahou R, Hidas G, Duvdevani M, Sosna J (2010) Determination of renal stone composition with dual-energy computed tomography: an emerging application. Semin Ultrasound CT MRI. 31(4):315–320
35. Boll DT, Patil NA, Paulson EK, et al. (2009) Renal stone assessment with dual-energy multidetector CT and advanced postprocessing techniques: improved characterization of renal stone composition—pilot study 1. Radiology. 250(3):813–820
36. Matlaga BR, Kawamoto S, Fishman E (2008) Dual source computed tomography: a novel technique to determine stone composition. Urology. 72(5):1164–1168
37. Stolzmann P, Kozomara M, Chuck N, et al. (2010) In vivo identification of uric acid stones with dual-energy CT: diagnostic performance evaluation in patients. Abdom Imaging. 35(5):629–635
38. Primak AN, Fletcher JG, Vrtiska TJ, et al. (2007) Noninvasive differentiation of uric acid versus non-uric acid kidney stones using dual-energy CT. Acad Radiol. 14(12):1441–1447
39. Tamm EP, Le O, Liu X, et al. (2017) "How to" incorporate dual energy imaging into a high volume abdominal imaging practice. Abdom Radiol N Y. 42(3):688–701
40. Van Der Kooy K, Leenen R, Seidell JC, Deurenberg P, Visser M (1993) Abdominal diameters as indicators of visceral fat: comparison between magnetic resonance imaging and anthropometry. Br J Nutr. 70(01):47